ELSEVIER

International Journal of Solids and Structures 41 (2004) 907–921

INTERNATIONAL JOURNAL OF SOLIDS and STRUCTURES

www.elsevier.com/locate/ijsolstr

Energy release rate and path independent integral study for piezoelectric material with crack

C.P. Spyropoulos *

Department of Mechanics, National Technical University of Athens, Zografou Campus, Theocaris Bld, Gr. 15773 Athens, Greece

Received 21 April 2003

Abstract

The concept that an excess of energy would be required to extend a segment of the crack has been widely accepted and applied to characterize crack extension behavior for isotropic and homogeneous materials at the macroscopic scale. For linear elastic materials, the path independent integral is basically the same as that of energy release rate.

Fracture analyses of multifunctional materials that involve mechanical as well as electric energy, however, show that inconsistencies could arise when applying the energy release rate or the path independent integral as a criterion of fracture. A sign change in the computed energy release rate could occur depending on the specified boundary conditions. This means that crack extension could correspond to dissipation as well as absorption of energy. Although this result has been pointed out in earlier publications but the implications have not been fully explored.

In order to focus attention on the objective of this work, a simplified formulation of the piezoelectric crack problem will be considered. It will contain only three material constants. As it has been shown in previous works, the simplified piezoelastic solutions would exhibit the same qualitative conclusions. Results are presented for poling directed normal and parallel to the line crack. Shown specifically is the energy release rate can change sign as the applied mechanical stress is altered in relation to the applied electric field.

1. Introduction

Studies concerned with the fracture of piezoceramic materials have had continuing interest in the literature for many years, both theoretically (McMeeking, 1990; Li et al., 1990; Gao and Barnett, 1996) and experimentally (Pak and Tobin, 1993; Tobin and Pak, 1993; Park and Sun, 1995). They are too numerous to be listed. Among the papers that stand out as being original in finding parameters for characterizing the fracture behavior of piezoelectric materials are those of Gao et al. (1997) and Suo et al. (1992). Derived by Suo et al. (1992) is a path independent integral J for the piezoelectric material in contrast to the original J-integral derived by Rice (1968) for the isotropic (elastic) material that could be nonlinear but still elastic. That is it could be applied to the theory of deformation plasticity. Budiansky and Rice

* Tel.: +30-210-7721305; fax: +30-210-7721302.
E-mail address: cspyrop@central.ntua.gr (C.P. Spyropoulos).

0020-7683/$ - see front matter © 2003 Elsevier Ltd. All rights reserved.
doi:10.1016/j.ijsolstr.2003.09.031

(1973) attempted to extend the use of path independent integrals by introducing other integrals referred to as L and M but their physical meaning in terms of fracture was not clear even though they have been expounded extensively by others (Chen and Ma, 1997; Herrmann and Herrmann, 1981; Chen and Hasebe, 1998; Chen and Lu, 2001). One of the objectives of the present work is to point out the need to understand whether it is possible to have a negative energy release rate as it was raised in the paper by Gao et al. (1997). Obviously, some basic experiments should be done to provide some insights to this problem. The continuing publication of results related to J, L or M integrals for different crack configurations serves little or no purpose.

There are alternate choices for fracture criteria. One of them is the strain energy density factor criterion (Zuo and Sih, 2000; Sih and Zuo, 2000; Sih and Song, 2002; Song and Sih, 2002). It has the advantage that it is always positive and does not encounter the difficulties to explain that the crack tip would release energy at one time and absorb energy at other times. What the strain energy density criterion has already done is to have explained the phenomenon of crack growth enhancement and retardation when the direction of the applied electric field is changed relative to that of poling (Zuo and Sih, 2000; Sih and Zuo, 2000; Spyropoulos et al., 2002). The energy release rate expression could not explain this phenomenon when the direction of poling is reversed.

2. Simplified formulation of piezoelasticity

In order to facilitate the computation of the energy release rate quantity, the classical piezoelastic equations will be approximated and simplified for solving crack problems. It is assumed that the displacement in the material parallel to the crack is negligibly small in comparison with that normal to the crack in a two-dimensional space. This approach was first introduced by Rice et al. (1994) and later was used in conjunction with complex functions (Gao et al., 1997; Sih, 2002).

Considered is a crack with length $2a$ that lies on x-axis centered at the origin of coordinate as shown in Fig. 1. Mechanical stress σ_∞ or strain ϵ_∞ are applied to the medium at distance remote from the crack. Electric field E_∞ or electric displacement D_∞ can also be applied as shown in Fig. 1(a) for poling normal to the crack and in Fig. 1(b) for poling parallel to the crack. In the former case, there prevails a transverse stress $\sigma_x^\infty = eE_y^\infty$. Here, e stands for one of the piezoelectric constants of the materials. The simplified version of the displacement field can be written as

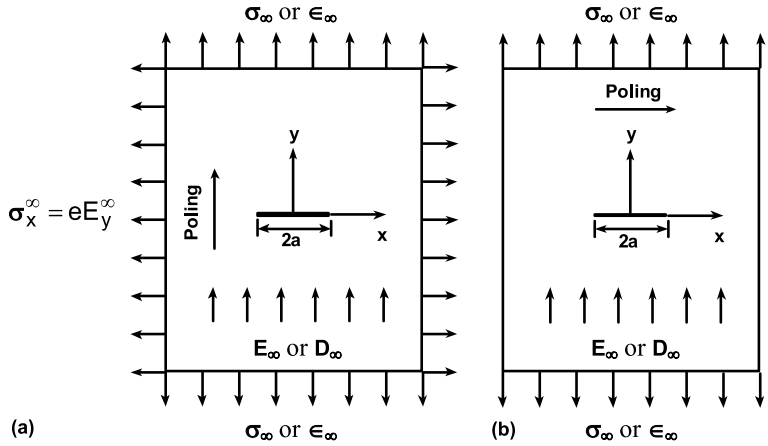

Fig. 1. Boundary conditions and poling directions: (a) poling normal to crack and (b) poling parallel to crack.

$$u_x = 0, \quad u_y = u(x,y) \tag{1}$$

The electric field components E_x and E_y can be expressed in terms of an electric potential function $\phi(x,y)$ as

$$E_x = -\phi_{,x}, \quad E_y = -\phi_{,y} \tag{2}$$

where comma refers to differentiation with respect to the space variables. The boundary condition on crack surface can be written as

$$\sigma_y = 0, \quad D_y = 0 \quad \text{for } -a < x < a;\ y = 0 \tag{3}$$

2.1. Poling normal to crack

If the poling direction coincides with the y-axis, then the constituent relations are given by

$$\sigma_x = -e\phi_{,y}, \quad \sigma_y = (mu + e\phi)_{,y}, \quad \sigma_{xy} = (mu + e\phi)_{,x} \tag{4}$$

$$D_x = (eu - \varepsilon\phi)_{,x}, \quad D_y = (eu - \varepsilon\phi)_{,y} \tag{5}$$

Refer to Gao et al. (1997) and Sih (2002) for details. In the absence of body force and body charge, the governing field equations become

$$\nabla^2 u = 0, \quad \nabla^2 \phi = 0 \tag{6}$$

in which ∇^2 is the Laplacian operator in two-dimensions.

According to Eq. (6), the displacement and electric potential functions can be expressed in terms of two complex functions of the variable $z = x + \mathrm{i}y$ as

$$u = \mathrm{Im}[\Omega(z)], \quad \phi = \mathrm{Im}[\Phi(z)]. \tag{7}$$

It follows that the stress and electric displacement components are given by

$$\begin{aligned} \sigma_y + \mathbf{i}\sigma_{xy} &= m\Omega'(z) + e\Phi'(z) \\ D_y + \mathbf{i}D_x &= e\Omega'(z) - \varepsilon\Phi'(z) \end{aligned} \tag{8}$$

For an embedded line crack, the potential functions $\Omega(z)$ and $\Phi(z)$ take the form

$$\Omega(z) = A\sqrt{z^2 - a^2}, \quad \Phi(z) = B\sqrt{z^2 - a^2} \tag{9}$$

The crack surface conditions in Eq. (3) are thus satisfied. The constants A and B are required to be real. They can be determined from the boundary conditions at infinity. Without going into details, the asymptotic field solution can be written as

$$\begin{aligned} &\sigma_y = (mA + eB)\sqrt{\frac{a}{2r}}\cos\frac{\theta}{2}, \quad \sigma_{xy} = -(mA + eB)\sqrt{\frac{a}{2r}}\sin\frac{\theta}{2}, \quad \sigma_x = -eB\sqrt{\frac{a}{2r}}\cos\frac{\theta}{2} \\ &D_y = (eA - \varepsilon B)\sqrt{\frac{a}{2r}}\cos\frac{\theta}{2}, \quad D_x = -(eA - \varepsilon B)\sqrt{\frac{a}{2r}}\sin\frac{\theta}{2} \end{aligned} \tag{10}$$

The total energy density function W is

$$W = \frac{1}{2}\sigma_{ij}\epsilon_{ij} + \frac{1}{2}D_i E_i = \frac{a(mA^2 + \varepsilon B^2)}{4r} \tag{11}$$

The J-integral originally derived by Rice (1968) is given by

$$J_M = \oint_C \left(W\,\mathrm{d}x - \sigma_{ij} n_j \frac{\partial u_i}{\partial x}\,\mathrm{d}s \right) = \frac{a\pi}{2} A(mA + eB) \tag{12}$$

while the energy release rate using crack enclosure procedure as proposed by Irwin takes the form

$$G_M = \frac{1}{2} \operatorname*{Lim}_{\delta a \to 0} \frac{1}{\delta a} \int_0^{\delta a} \sigma_{yi}(a + x) u_i(a - \delta a + x)\,\mathrm{d}x = \frac{a\pi}{2} A(mA + eB) \tag{13}$$

The modified J-integral for piezoelasticity can be found in Suo et al. (1992) and it is designated as

$$J_1 = \oint_C \left[(W - D_i E_i) n_x - \sigma_{ij} n_j \frac{\partial u_i}{\partial x} - n_i D_i \phi_{,x} \right] \mathrm{d}s = \frac{a\pi}{2} (mA^2 + 2eAB - \varepsilon B^2) \tag{14}$$

$$J_2 = \oint_C \left[(W - D_i E_i) n_y - \sigma_{ij} n_j \frac{\partial u_i}{\partial y} - n_i D_i \phi_{,y} \right] \mathrm{d}s = 0 \tag{15}$$

in which the subscripts $i, j = x, y$. Similarly, a modified energy release rate for piezoelasticity is

$$\begin{aligned} G &= \frac{1}{2} \operatorname*{Lim}_{\delta a \to 0} \frac{1}{\delta a} \int_0^{\delta a} \left[\sigma_{yi}(a + x) u_i(a - \delta a + x) + D_y(a + x) \phi(a - \delta a + x) \right] \mathrm{d}x \\ &= \frac{a\pi}{2} (mA^2 + 2eAB - \varepsilon B^2) \end{aligned} \tag{16}$$

It can be seen that G and J are essentially the same

$$G = J_1, \quad G_M = J_M \tag{17}$$

The first and second expressions in Eq. (17) correspond, respectively, to the modified (piezoelasticity) and unmodified (elasticity) version of the energy release rate.

2.2. Poling parallel to crack

When the poling direction is along the x-axis, the constituent relations take another form

$$\sigma_x = e\phi_{,x}, \quad \sigma_y = mu_{,y} - e\phi_{,x}, \quad \sigma_{xy} = mu_{,x} + e\phi_{,y} \tag{18}$$

$$D_x = -eu_{,y} - \varepsilon\phi_{,x} \quad D_y = eu_{,x} - \varepsilon\phi_{,y} \tag{19}$$

The governing field equations remain unchanged

$$\nabla^2 u = 0, \quad \nabla^2 \phi = 0 \tag{20}$$

The displacement and electric potential functions can again be expressed in terms of complex functions:

$$u = \mathrm{Re}[U(z)], \quad \phi = \mathrm{Im}[V(z)] \tag{21}$$

The stress and electric displacement components become

$$\begin{aligned} \sigma_{xy} - \mathbf{i}\sigma_y &= mU'(z) + eV'(z) \\ D_y + \mathbf{i}D_x &= eU'(z) - \varepsilon V'(z) \end{aligned} \tag{22}$$

According to the boundary conditions on the crack surface, the potential functions $U(z)$ and $V(z)$ can be written as

$$mU'(z)+eV'(z)=\frac{Az\mathbf{i}}{\sqrt{z^2-a^2}},\quad eU'(z)-\varepsilon V'(z)=\frac{Bz}{\sqrt{z^2-a^2}}+C\mathbf{i} \tag{23}$$

Assume $\sigma_x^{\infty}=0$, such that constant C in above equation can be determined as $C=eA/m$.

The asymptotic field solution is

$$\begin{aligned}\sigma_y&=-A\sqrt{\frac{a}{2r}}\cos\frac{\theta}{2},\quad \sigma_{xy}=A\sqrt{\frac{a}{2r}}\sin\frac{\theta}{2}\\ D_y&=B\sqrt{\frac{a}{2r}}\cos\frac{\theta}{2},\quad D_x=-B\sqrt{\frac{a}{2r}}\sin\frac{\theta}{2}\end{aligned} \tag{24}$$

It can be shown that the total energy density W takes the form

$$W=\frac{1}{2}\sigma_{ij}\epsilon_{ij}+\frac{1}{2}D_iE_i=\frac{a(\varepsilon A^2+mB^2)}{4r(m\varepsilon+e^2)} \tag{25}$$

As for the case of poling normal to the crack J_M and G_M can be computed as

$$J_M=\oint_C\left(W\,\mathrm{d}x-\sigma_{ij}n_j\frac{\partial u_i}{\partial x}\,\mathrm{d}s\right)=\frac{a\pi\varepsilon}{2(m\varepsilon+e^2)}A^2 \tag{26}$$

$$G_M=\frac{1}{2}\operatorname*{Lim}_{\delta a\to 0}\frac{1}{\delta a}\int_0^{\delta a}\sigma_{yi}(a+x)u_i(a-\delta a+x)\,\mathrm{d}x=\frac{a\pi\varepsilon}{2(m\varepsilon+e^2)}A^2 \tag{27}$$

The modified J-integrals in Suo et al. (1992) are given by

$$J_1=\oint_C\left[(W-D_iE_i)n_x-\sigma_{ij}n_j\frac{\partial u_i}{\partial x}-n_iD_i\phi_{,x}\right]\mathrm{d}s=\frac{a\pi}{2(m\varepsilon+e^2)}(\varepsilon A^2-mB^2) \tag{28}$$

$$J_2=\oint_C\left[(W-D_iE_i)n_y-\sigma_{ij}n_j\frac{\partial u_i}{\partial y}-n_iD_i\phi_{,y}\right]\mathrm{d}s=0 \tag{29}$$

The modified energy release rate is

$$\begin{aligned}G&=\frac{1}{2}\operatorname*{Lim}_{\delta a\to 0}\frac{1}{\delta a}\int_0^{\delta a}\left[\sigma_{yi}(a+x)u_i(a-\delta a+x)+D_y(a+x)\phi(a-\delta a+x)\right]\mathrm{d}x\\ &=\frac{a\pi}{2(m\varepsilon+e^2)}(\varepsilon A^2-mB^2)\end{aligned} \tag{30}$$

According to the above results, the relations in Eq. (17) are again established.

3. Stress/strain and electric field/displacement boundary conditions

The response of piezoceramics depends sensitively on the stress/strain and electric field/displacement boundary conditions. According to the work of Sih (2002), eight possible cases can be considered. They are given in Table 1 as Case numbers I, II, …,VIII. The first four referred to as the natural boundary conditions and the last four as the mixed boundary conditions.

For each case, the parameters A and B in Eqs. (11)–(16) for poling normal to the crack will be different from those in Eqs. (25)–(30) for poling parallel to the crack. They are given in Tables 2 and 3.

Table 1
Classification of boundary conditions (Sih, 2002)

Case no.	Poling reference to crack	Boundary conditions	Transverse constraint
Natural boundary conditions			
I	Normal	$(\sigma_\infty, E_\infty)$	$\sigma_x^\infty = eE_y^\infty$
II	Parallel	$(\sigma_\infty, E_\infty)$	$\sigma_x^\infty = 0$
III	Normal	$(\epsilon_\infty, E_\infty)$	$\sigma_x^\infty = eE_y^\infty$
IV	Parallel	$(\epsilon_\infty, E_\infty)$	$\sigma_x^\infty = 0$
Mixed boundary conditions			
V	Normal	$(\sigma_\infty, D_\infty)$	$\sigma_x^\infty = eE_y^\infty$
VI	Parallel	$(\sigma_\infty, D_\infty)$	$\sigma_x^\infty = 0$
VII	Normal	$(\epsilon_\infty, D_\infty)$	$\sigma_x^\infty = eE_y^\infty$
VIII	Parallel	$(\epsilon_\infty, D_\infty)$	$\sigma_x^\infty = 0$

Table 2
Parameters A and B for pole normal to crack

Case no.	Constants	
	A	B
I	$(\sigma_\infty + eE_\infty)/m$	$-E_\infty$
III	ϵ_∞	$-E_\infty$
V	$(\epsilon\sigma_\infty + eD_\infty)/(m\varepsilon + e^2)$	$(e\sigma_\infty - mD_\infty)/(m\varepsilon + e^2)$
VII	ϵ_∞	$(e\epsilon_\infty - D_\infty)/\varepsilon$

Table 3
Parameters A and B for pole parallel to crack

Case no.	Constants	
	A	B
II	$-\sigma_\infty$	$(m\varepsilon + e^2)/mE_\infty$
IV	$-m\epsilon_\infty$	$(m\varepsilon + e^2)/mE_\infty$
VI	$-\sigma_\infty$	D_∞
VIII	$-m\epsilon_\infty$	D_∞

3.1. Normal poling

Substituting the results of Table 2 into the expressions for J and J_M, the equivalent energy release rates are obtained.

- *Case I* (σ_∞ *and* E_∞)

$$J = \frac{a\pi}{2m}[\sigma_\infty^2 - (m\varepsilon + e^2)E_\infty^2] \tag{31}$$

$$J_M = \frac{a\pi}{2m}\sigma_\infty(\sigma_\infty + eE_\infty) \tag{32}$$

- *Case III* (ϵ_∞ *and* E_∞)

$$J = \frac{a\pi}{2}(m\epsilon_\infty^2 - 2eE_\infty\epsilon_\infty - \varepsilon E_\infty^2) \tag{33}$$

$$J_M = \frac{a\pi}{2}\epsilon_\infty(m\epsilon_\infty - eE_\infty) \tag{34}$$

- *Case V* (σ_∞ *and* D_∞)

$$J = \frac{a\pi}{2(m\varepsilon + e^2)}(\varepsilon\sigma_\infty^2 + 2e\sigma_\infty D_\infty - mD_\infty^2) \tag{35}$$

$$J_M = \frac{a\pi}{2(m\varepsilon + e^2)}\sigma_\infty(\varepsilon\sigma_\infty + eD_\infty) \tag{36}$$

- *Case VII* (ϵ_∞ *and* D_∞)

$$J = \frac{a\pi}{2\varepsilon}[(\varepsilon m + e^2)\epsilon_\infty^2 - D_\infty^2] \tag{37}$$

$$J_M = \frac{a\pi}{2\varepsilon}\epsilon_\infty[(\varepsilon m + e^2)\epsilon_\infty - eD_\infty] \tag{38}$$

It is not difficult to conclude from the above that when the mechanical applied stress σ_∞ or applied strain ϵ_∞ become vanishingly small, J_M in Eqs. (32), (34), (36) and (38) tend to zero while the Js in Eqs. (31), (33), (35) and (37) become negative. Negative J or G cannot be explained on physical grounds, at least not by this model. According to the conventional fracture mechanics interpretation, a negative J or G would correspond to a crack that could absorb energy instead of giving off energy to the surrounding as a result of lost surface energy due to crack extension.

Even though J_M vanished with the mechanical applied stress and strain, it is not obvious that it should be regarded as the mechanical energy release (Park and Sun, 1995) since Eqs. (32) and (34) do contain the electric field E_∞ and Eqs. (36) and (38) contain the electric displacement D_∞. In other words, electrical energy is contained in J_M.

3.2. Parallel poling

In the same way, the parameters A and B in Table 3 can be substituted into Eqs. (26) and (28) to yield the J_M and J expressions for poling aligned parallel to the crack. The results are

- *Case II* (σ_∞ *and* E_∞)

$$J = \frac{a\pi}{2(m\varepsilon + e^2)}\left[\varepsilon\sigma_\infty^2 - \frac{(m\varepsilon + e^2)^2}{m}E_\infty^2\right] \tag{39}$$

$$J_M = \frac{a\pi\varepsilon}{2(m\varepsilon + e^2)}\sigma_\infty^2 \tag{40}$$

- *Case IV* (ϵ_∞ *and* E_∞)

$$J = \frac{a\pi}{2(m\varepsilon + e^2)}\left[\varepsilon m^2\epsilon_\infty^2 - \frac{(m\varepsilon + e^2)^2}{m}E_\infty^2\right] \tag{41}$$

$$J_M = \frac{a\pi\varepsilon m^2}{2(m\varepsilon + e^2)}\epsilon_\infty^2 \tag{42}$$

- *Case VI* (σ_∞ *and* D_∞)

$$J = \frac{a\pi}{2(m\varepsilon + e^2)}[\varepsilon\sigma_\infty^2 - mD_\infty^2] \tag{43}$$

$$J_M = \frac{a\pi\varepsilon}{2(m\varepsilon + e^2)}\sigma_\infty^2 \tag{44}$$

- *Case VIII* (ϵ_∞ *and* D_∞)

$$J = \frac{a\pi m}{2(m\varepsilon + e^2)}[\varepsilon m\epsilon_\infty^2 - D_\infty^2] \tag{45}$$

$$J_M = \frac{a\pi\varepsilon m^2}{2(m\varepsilon + e^2)}\epsilon_\infty^2 \tag{46}$$

It can again be seen that when mechanical loads are absent J in Eqs. (39), (41), (43) and (45) become negative. This is contrary to the energy release rate fracture model where energy is assumed to be transferred from the system with a crack to the surrounding rather than the opposite. The quantity J_M in Eqs. (40), (42), (44) and (46) vanish. As emphasized earlier, this does not imply that J_M is associated exclusively with mechanical loading.

4. Discussion of numerical results for PZT-4 piezoceramic

To compare the results of the present investigation with those in Sih (2002), calculations will be made for the PZT-4 piezoceramic material. For the simplified formulation, the constants in Table 4 will be averaged as in Sih (2002) to yield $m = 6.93 \times 10^{10}$ N/m^2, $e = 13.64$ C/m^2 and $\varepsilon = 5.74 \times 10^{-9}$ C/Vm. Using these

Table 4
Material properties of PZT-4 piezoceramic

Elastic constants $\times 10^{10}$ (N/m^2)				Piezoelectric constants (C/m^2)			Dielectric permittivities $\times 10^{-9}$ (C/V m)	
c_{11}	c_{13}	c_{33}	c_{44}	e_{31}	e_{33}	e_{15}	ε_{11}	ε_{33}
13.9	7.43	11.3	2.56	−6.98	13.84	13.44	6.00	5.47

Table 5
Numerical data for Cases I and II

p_σ (V m/N)	Case I			Case II		
	$J/(a\sigma_\infty^2/m)$	$J_M/(a\sigma_\infty^2/m)$	$S/(a\sigma_\infty^2/m)$	$J/(a\sigma_\infty^2/m)$	$J_M/(a\sigma_\infty^2/m)$	$S/(a\sigma_\infty^2/m)$
−0.08	−4.30	−0.14	0.64	−4.80	1.07	1.10
−0.04	0.10	0.71	0.21	−0.40	1.07	0.40
−0.02	1.20	1.14	0.17	0.70	1.07	0.23
−0.01	1.48	1.36	0.20	0.98	1.07	0.18
0.00	1.57	1.57	0.25	1.07	1.07	0.17
0.01	1.48	1.79	0.33	0.98	1.07	0.18
0.02	1.20	2.00	0.44	0.70	1.07	0.23
0.04	0.10	2.43	0.76	−0.40	1.07	0.40
0.08	−4.30	3.28	1.73	−4.80	1.07	1.10

value, J and J_M will be computed for Cases I, II, ..., VIII and compared with those given in Sih (2002) for the energy density factor S. Refer to Table 5 for Cases I and II; Table 6 for Cases III and IV; Table 7 for Case V and VI; and Table 8 for Cases VII and VIII.

The numerical values of J, J_M and S for Case I and II in Table 5 are calculated for different σ_∞ and E_∞ or the ratio $p_\sigma = E_\infty/\sigma_\infty$. They are normalized as shown in Table 5 and plotted in Fig. 2 for Case I. Note that the curves for J and J_M can be negative depending on p_σ. The curve for J is positive for values of p_σ between -0.042 and $+0.042$. The curve is symmetric. Outside of the above range J becomes negative for $p_\sigma < -0.042$ and $p_\sigma > +0.042$. Similarly, J_M switches from positive to negative value at $p_\sigma \approx -0.074$. Only the normalized S-curve remains positive for all values of p_σ and does not encounter difficulties in physical reasoning.

Table 5 also gives the numerical results for Case II, a graphical representation of which is displayed in Fig. 3. Both the normalized J_M and S are positive but again J can be negative for $p_\sigma < -0.034$ and $p_\sigma > +0.034$. This shows that the range of E_∞/σ_∞ for which J is positive is very small.

Results for Cases III and IV in Table 6 are summarized graphically in Figs. 4 and 5, respectively. The unmodified path independent integral J_M is positive until the applied electric field E_∞ to applied strain ϵ_∞ ratio p_ε reaches about $+0.51\times10^{10}$at which point J_M takes on negative values. Fig. 4 also shows that the modified integral J is positive only in the range $-0.67 \times 10^{10} < p_\varepsilon < +0.18 \times 10^{10}$. The range for positive J narrows down to $-0.22 \times 10^{10} < p_\varepsilon < +0.22 \times 10^{10}$ for Case IV in Fig. 5 while $J_M/[am(\epsilon_\infty)^2]$ and $S/[am(\epsilon_\infty)^2]$ remain positive for all p_ε.

Table 6
Numerical data for Cases III and IV

$p_\varepsilon \times 10^{10}$ (V/m)	Case III			Case IV		
	$J/(am\epsilon_\infty^2)$	$J_M/(am\epsilon_\infty^2)$	$S/(am\epsilon_\infty^2)$	$J/(am\epsilon_\infty^2)$	$J_M/(am\epsilon_\infty^2)$	$S/(am\epsilon_\infty^2)$
−0.8	−1.81	4.04	1.58	−11.15	1.07	2.12
−0.5	1.41	3.12	0.77	−3.70	1.07	0.93
−0.2	2.29	2.19	0.33	0.31	1.07	0.29
−0.1	2.06	1.88	0.27	0.88	1.07	0.20
0.0	1.57	1.57	0.25	1.07	1.07	0.17
0.1	0.82	1.26	0.27	0.88	1.07	0.20
0.2	−0.19	0.95	0.33	0.31	1.07	0.29
0.5	−4.77	0.02	0.77	−3.70	1.07	0.93
0.8	−11.70	−0.90	1.58	−11.15	1.07	2.12

Table 7
Numerical data for Cases V and VI

$q_\sigma \times 10^{-10}$ (C/N)	Case V			Case VI		
	$J/(a\sigma_\infty^2/m)$	$J_M/(a\sigma_\infty^2/m)$	$S/(a\sigma_\infty^2/m)$	$J/(a\sigma_\infty^2/m)$	$J_M/(a\sigma_\infty^2/m)$	$S/(a\sigma_\infty^2/m)$
−6.0	−6.63	−0.46	0.91	−3.58	1.07	0.91
−3.0	−1.62	0.31	0.36	−0.09	1.07	0.36
−2.0	−0.46	0.56	0.25	0.55	1.07	0.25
−1.0	0.43	0.82	0.19	0.94	1.07	0.19
0.0	1.07	1.07	0.17	1.047	1.07	0.17
1.0	1.45	1.32	0.19	0.94	1.07	0.19
2.0	1.57	1.58	0.25	0.55	1.07	0.25
3.0	1.43	1.83	0.36	−0.09	1.07	0.36
6.0	−0.53	2.60	0.91	−3.58	1.07	0.91

Table 8
Numerical data for Cases VII and VIII

q_e (C/m^2)	Case VII			Case VIII		
	$J/(am\epsilon_\infty^2)$	$J_M/(am\epsilon_\infty^2)$	$S/(am\epsilon_\infty^2)$	$J/(am\epsilon_\infty^2)$	$J_M/(am\epsilon_\infty^2)$	$S/(am\epsilon_\infty^2)$
−50	−7.57	5.0	2.80	−5.66	1.07	1.24
−30	−1.25	3.92	1.45	−1.35	1.07	0.56
−20	0.73	3.38	0.96	−0.01	1.07	0.34
−10	1.91	2.84	0.60	0.80	1.07	0.21
0.0	2.31	2.31	0.37	1.07	1.07	0.17
10	1.91	1.77	0.26	0.80	1.07	0.21
20	0.73	1.23	0.28	−0.01	1.07	0.34
30	−1.25	0.69	0.42	−1.35	1.07	0.56
50	−7.57	−0.39	1.08	−5.66	1.07	1.24

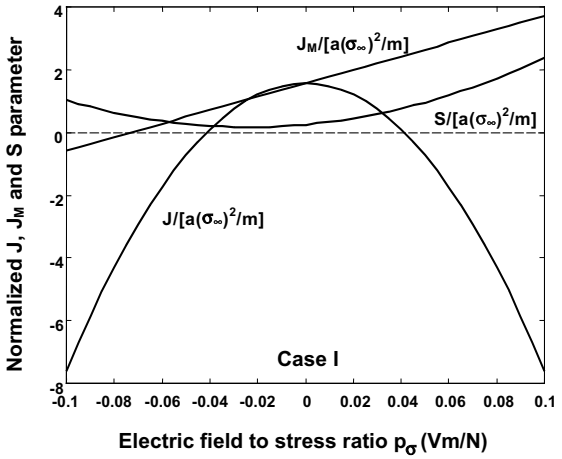

Fig. 2. Normalized J, J_M and S parameters as fracture criteria for Case I with p_σ specified.

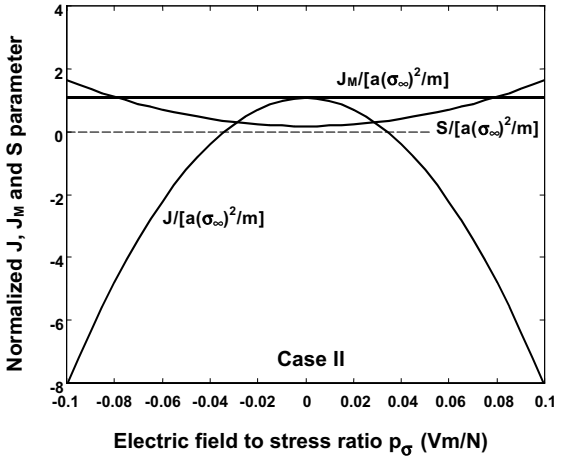

Fig. 3. Normalized J, J_M and S parameters as fracture criteria for Case II with p_σ specified.

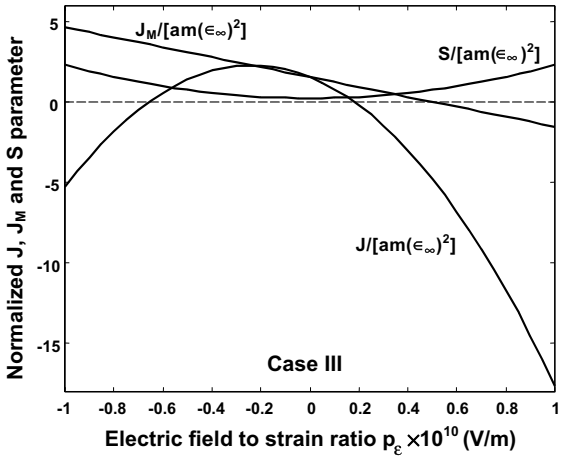

Fig. 4. Normalized J, J_M and S parameters as fracture criteria for Case III with p_ε specified.

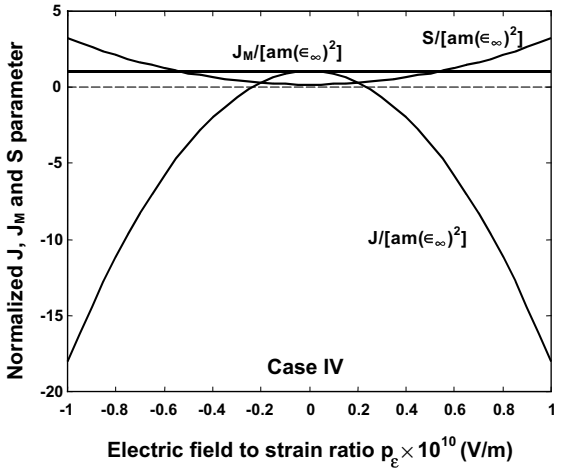

Fig. 5. Normalized J, J_M and S parameters as fracture criteria for Case IV with p_ε specified.

The curves in Figs. 6 and 7 for Cases V and VI of Table 7 are similar to those for Cases I and II in Table 5. Note that J_M in Fig. 6 would change sign at $q_\sigma \cong -4.2 \times 10^{-10}$ C/N where $q_\sigma = D_\infty/\sigma_\infty$ with D_∞ being the uniform electric displacement far away from the crack. The range for J being positive is $-1.60 \times 10^{-10} < q_\sigma < +5.40 \times 10^{-10}$ C/N. The trend of the curves in Fig. 7 for q_σ is the same as that in Fig. 3 for p_σ. In Fig. 7, only J becomes negative for $q_\sigma < -2.9 \times 10^{-10}$ C/N and $q_\sigma > 2.9 \times 10^{-10}$ C/N. The normalized energy density factor remained positive for all q_σ in Figs. 6 and 7.

The data in Table 8 correspond to the specification of D_∞ and ϵ_∞ for Cases VII and VIII. When $q_\varepsilon = D_\infty/\epsilon_\infty$ is specified, the resulting curves are exhibited in Figs. 8 and 9 and they are qualitatively the same as those in Figs. 4 and 5 for Cases III and IV. The point where J_M in Fig. 8 changes sign occurs at $q_\varepsilon \approx 43$ C/m^2 and the range for which J remains positive is $-24.0 < q_\varepsilon < 24.0$ C/m^2. By the same token, Fig. 9 shows that both J_M and S are positive for all q_ε while J is positive only in the range $-20.0 < q_\varepsilon < 20.0$ C/m^2.

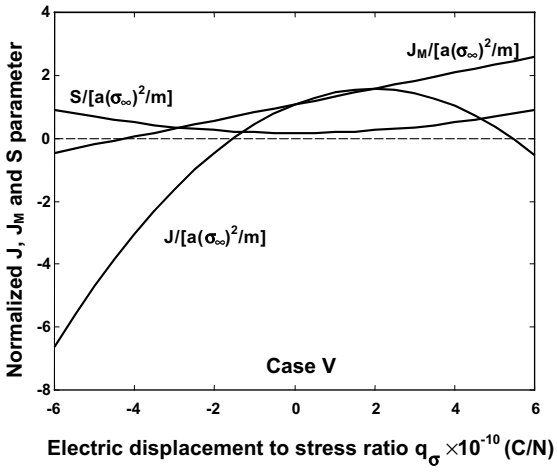

Fig. 6. Normalized J, J_M and S parameters as fracture criteria for Case V with q_σ specified.

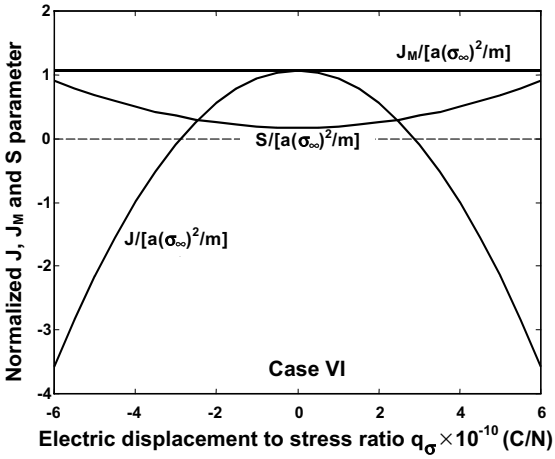

Fig. 7. Normalized J, J_M and S parameters as fracture criteria for Case VI with q_σ specified.

5. Concluding remarks and future work

The path independent J-integral has been used in fracture mechanics based on the premise that it is connected with the energy released by a unit extension of a line crack. It is limited to nonlinear elastic materials and serves a useful purpose for evaluating the local stress field of a "conservative" system. When energy dissipation occurs, the concept serves little or no purpose. Use of the energy dissipation function becomes necessary. This point has been well documented in Sih (1988) and Sih (1992) related to the isoenergy density theory and Mast et al. (1995) for actually measuring the energy dissipation function for composites. The dissipation function measured in Mast et al. (1995) coincides with that used in the isoenergy density theory in Sih (1988) and Sih (1992).

This work attempts to better understand whether the path independent integral and energy release rate tool could be applied without controversy to multiscale energy transfer rate crack problems. A particular

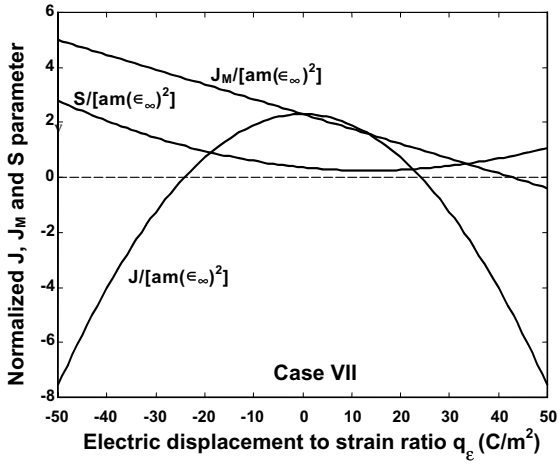

Fig. 8. Normalized J, J_M and S parameters as fracture criteria for Case VII with q_ε specified.

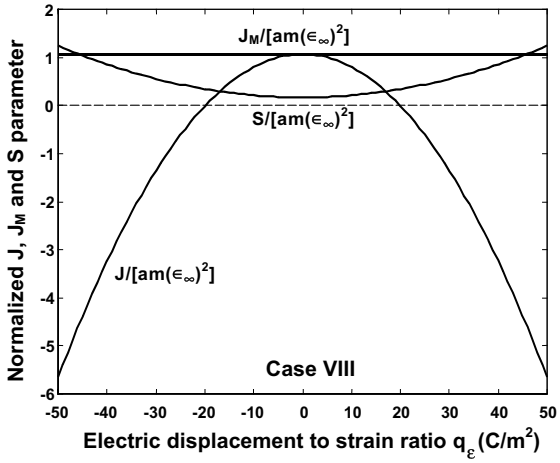

Fig. 9. Normalized J, J_M and S parameters as fracture criteria for Case VIII with q_ε specified.

situation would be the simultaneous application of electrical and mechanical energy. The theory of linear piezoelasticity is thus applied to test the validity of the so referred to J_k $(k = 1, 2)$ and J-integral in the literature beyond isotropic elasticity. It is disturbing to find that both J_k (or J_1) and J for a crack can switch sign for different value of the applied electric field E_∞ and electric displacement D_∞ in relation to the applied mechanical stress σ_∞ and strain ϵ_∞. It depends on the prevailing boundary conditions. Previous works related to J-integrals were limited to simple materials and boundary conditions. The simple formulation adopted in this work provides closed form solutions to complicated boundary value problems for testing the validity of J or J_k. It is important to know whether they will remain valid when they are applied to piezoelectric materials. The objective is to test whether J or J_k could be used as a fracture criterion other than idealized isotropic elastic systems where the energy release rate is limited to a crack segment the length of which is assumed to vanish in the limit. To this end, it has been shown conclusively that J or J_k deny

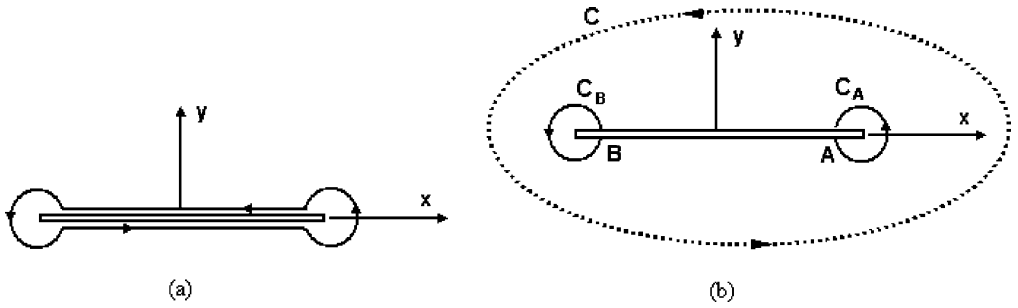

Fig. 10. Contours of integration: (a) closed contour and (b) open contour.

positive energy release for the specification of the applied electric field E_∞ and electric displacement D_∞ when no mechanical stress σ_∞ and strain ϵ_∞ are applied. The validity or invalidity could then be decided by an experiment where only E_∞ is applied with σ_∞ (and ϵ_∞) equal to zero. If a crack could be extended (corresponding to positive energy release), then the experiment would contradict the validity of J and J_k where they are predicted to be negative.

For the eight different boundary conditions examined, J integral tends to increase in the negative direction as the applied electric field is increased. This implies that there is less chance of fracturing a precracked piezoelectric specimen as the intensity of the applied electric field is increased. This conclusion does not seem to make physical sense. The same type of tests could be done to show whether a crack in piezoceramics would extend for values of E_∞ where J_M is predicted to be negative.

It also should be reiterated that regardless of whether the original J-integral (referred to as J_M in this work) is modified to J (or J_1) to include piezoelectricity or not they both could become negative. This is discomforting from the viewpoint of physics. Eq. (17) shows that J_1 and J_M are identical to the energy release rates G (modified) and G_M (Irwin's closure scheme), respectively. To further clarify the vanishing of J_2 in Eqs. (15) and (29) such that $J = J_1$ for a crack, reference can be made to the contours of integration in Fig. 10. Shrink the closed contour C in the integrals of Eqs. (15) and (29) onto the line crack as shown in Fig. 10(a). The line contours coinciding with the upper and lower crack surface would vanish because the crack is impermeable and free of tractions. Hence, the closed contour C reduces to two open contours C_A and C_B around the tips as shown in Fig. 10(b). Since $J_2^A = -J_2^B$, this gives $J_2^C = 0$ for poling parallel and normal to the crack. This gives the equivalent condition that $J = J_1$. In connection with this discussion, other path independent integrals have been studied in Budiansky and Rice (1973), Knowles and Sternberg (1972) and Chen (2001). They have been referred to as the L and M integrals and shown analytically to be related to energy release rates associated with crack rotation and expansion rates. Whether these proposed theoretical ideas could be used in fracture mechanics remain to be seen. Prior to using them in practical applications, they should pass the fundamental tests of not yielding contradictory results that are not permitted in mathematics. By the same token, the results could also not be validated by experiments.

Acknowledgements

The author wishes to thank Professor George C. Sih for his objective suggestions. They have broadened the outlook of the results of the manuscript in addition to ideas for future work. Helpful discussions have also been provided by my colleagues in the Department of Mechanics at the National Technical University of Athens. Their continuing assistance will be appreciated.

References

Budiansky, B., Rice, J.R., 1973. Conservation laws and energy release rates. ASME J. Appl. Mech. 40, 201–203.

Chen, Y.H., 2001. *M*-integral analysis for two-dimensional solids with strongly interacting microcracks. Parts in an infinite brittle solid. Int. J. Solids Struct. 38, 3193–3212.

Chen, Y.H., Hasebe, N., 1998. A consistency check for strongly interacting multiple crack problem in isotropic, anisotropic and bimaterial solids. Int. J. Fract. 89, 333–353.

Chen, Y.H., Lu, T.J., 2001. Conservation laws of the J_k-vector for microcrack damage in piezoelectric materials. Int. J. Solids Struct. 38, 3233–3249.

Chen, Y.H., Ma, H., 1997. Explicit formulation of the J_2- integral in anisotropic materials and its application in microcrack shielding problems. Sci. Chinese (E) 40 (6), 588–596.

Gao, H.J., Barnett, D.M., 1996. An invariance property of local energy release rates in a strip saturation model of piezoelectric fracture. Int. J. Fract. 79, 25–29.

Gao, H.J., Zhang, T.Y., Tong, P., 1997. Local and global energy release rates for an electrically yielded crack in a piezoelectric ceramic. J. Mech. Phys. Solids 45 (4), 491–510.

Herrmann, A.G., Herrmann, G., 1981. On energy release rates for a plane crack. ASME J. Appl. Mech. 48, 525–528.

Knowles, J.K., Sternberg, E., 1972. On a class of conservative laws in linearised and finite elastostatics. Arch. Rational Mech. Anal. 44 (3), 187–211.

Li, S., Cao, M., Cross, L.E., 1990. Stress and electric displacement distribution near Griffith's type III crack tips in piezoceramics. Mater. Lett. 10, 219–222.

Mast, P.W., Nash, G.E., Michopoulos, J., Thomas, R.W., Badaliance, R., Wolock, I., 1995. Characterization of strain induced damage in composites based on the dissipative energy density—Part I: basic scheme and formulation; Part II: composite specimens and naval structures; and Part III: general material constitutive relation. J. Theoret. Appl. Fract. Mech. 22 (2), 71–125.

McMeeking, R.M., 1990. A *J*-integral for the analysis of electrically induced mechanical stress at cracks in elastic dielectrics. Int. J. Eng. Sci. 28, 605–613.

Pak, Y.E., Tobin, A., 1993. On electric field effects in fracture of piezoelectric materials. In: Mechanics of Electromagnetic Materials and Structures, AMD-vol. 161/MD-vol.42. ASME, New York.

Park, S.B., Sun, C.T., 1995. Fracture criteria for piezoelectric ceramics. J. Am. Ceram. Soc. 78, 1475–1480.

Rice, J.R., 1968. A path independent integral and the approximate analysis of strain concentration by notches and cracks. ASME J. Appl. Mech. 35, 379–386.

Rice, J.R., Ben-Zion, Y., Kim, K.S., 1994. Three dimensional perturbative solution for a dynamic planar crack moving steadily in a model elastic solid. J. Mech. Phys. Solids 42, 813–843.

Sih, G.C., 1988. Thermomechanics of solids: nonequilibrium and irreversibility. J. Theoret. Appl. Fract. Mech. 9 (3), 175–198.

Sih, G.C., 1992. Some basic problems in non-equilibrium thermomechanics. In: Sienietyez, S., Salamon, P. Taylor and Francis, New York, pp. 218–247.

Sih, G.C., 2002. A field model interpretation of crack initiation and growth behavior in ferroelectric ceramics: change of poling direction and boundary condition. J. Theoret. Appl. Fract. Mech. 38 (1), 1–14.

Sih, G.C., Zuo, J.Z., 2000. Multiscale behavior of crack initiation and growth in piezoelectric ceramics. J. Theoret. Appl. Fract. Mech. 34 (2), 123–141.

Sih, G.C., Song, Z.F., 2002. Damage analysis of tetragonal perovskite structure ceramics implicated by asymptotic field solutions and boundary conditions. J. Theoret. Appl. Fract. Mech. 38 (1), 15–36.

Song, Z.F., Sih, G.C., 2002. Electromechanical influence of crack velocity at bifurcation for poled ferroelectric materials. J. Theoret. Appl. Fract. Mech. 38 (2), 121–139.

Spyropoulos, C.P., Song, Z.F., Ren, H.F., 2002. Nonuniform rate of crack growth in poled ferroelectric materials under anti-plane shear. In: Sih, G.C., Spyropoulos, C.P. (Eds.), International Symposium of Multiscaling in Mechanics. National Technical University of Athens Press, pp. 182–189.

Suo, Z., Kuo, C.M., Barnett, D.M., Willis, J.R., 1992. Fracture mechanics of piezoelectric ceramics. J. Mech. Phys. Solids 40, 739–765.

Tobin, A., Pak, Y.E., 1993. Effects of eletric fields on fracture behavior of PZT ceramics. In: Varadin, V.K. (Ed.), Smart Materials. In: SPIC, vol. 1916. ASME, New York, pp. 78–86. AMD vol. 161/MD vol. 42.

Zuo, J.Z., Sih, G.C., 2000. Energy density theory formulation and interpretation of cracking behavior for piezoelectric ceramics. J. Theoret. Appl. Fract. Mech. 34 (1), 17–33.